Chinese Chemical Letters 31 (2020) 1640–1643

Contents lists available at ScienceDirect

Chinese Chemical Letters

journal homepage: www.elsevier.com/locate/cclet

Communication

Different defect morphologies in polyethylene crystal induced by surface physicochemical properties

Yaqi Hou[a,c,d,*], Yi Ye[a,d], Zhongjie Du[d], Chen Zhang[d,**], Jianguo Mi[a,*], Xu Hou[b,c]

[a] State Key Laboratory of Organic-Inorganic Composites, Beijing University of Chemical Technology, Beijing 100029, China
[b] Research Institute for Soft Matter and Biomimetics, College of Physical Science and Technology, Xiamen University, Xiamen 361005, China
[c] State Key Laboratory of Physical Chemistry of Solid Surfaces, College of Chemistry and Chemical Engineering, Xiamen University, Xiamen 361005, China
[d] College of Materials Science and Engineering, Beijing University of Chemical Technology, Beijing 100029, China

ARTICLE INFO

Article history:
Received 4 June 2019
Received in revised form 16 July 2019
Accepted 25 July 2019
Available online 26 July 2019

Keywords:
Physicochemical properties
External surfaces
Defect morphologies
Polyethylene crystal
Dynamic density functional theory
Atomic scale

ABSTRACT

The physicochemical properties of surfaces have a great effect on the micro-morphologies of the crystal structures which are in contact with them. Understanding the interaction mechanism between the internal driving forces of the crystal and external inducing forces of the surfaces is the prerequisite of controlling and obtaining the desirable morphologies. In this work, the dynamic density functional theory was applied to construct the free energy functional expression of polyethylene (PE) lattice, and the micro-dynamic evolution processes of PE lattice morphology near the surfaces with different properties were observed to reveal the interaction mechanism at atomic scale. The results showed that the physical and chemical properties of the external surfaces synergistically affect the morphologies in both the defect shapes and the distribution of the defect regions. In the absence of the contact surfaces, driven by the oriented interactions among different CH_2 groups, PE lattices gradually grow and form a defect-free structure. Conversely, the presence of contact surfaces leads to lattice defects in the interfacial regions, and PE lattice shows different self-healing abilities around different surfaces.

© 2019 Chinese Chemical Society and Institute of Materia Medica, Chinese Academy of Medical Sciences. Published by Elsevier B.V. All rights reserved.

The existence of confinement effects, such as the addition of the external surfaces [1] or the confined spaces, such as nanochannels [2–4], will have great impacts on the microstructures and transport behaviors of the materials nearby or inside, which brings new properties and applications. For crystalline materials, controlling the crystal structure around an external surface to obtain desirable morphologies and properties is of both fundamental and technological importance [5,6]. The prerequisite of controlling is to clarify the interaction mechanism between the internal driving forces of the crystal and external inducing forces of the surfaces during the formation of the lattice. From the studies of amorphous materials, it has been proved that changing physicochemical properties of the external surfaces, hereinafter referred to as the surface properties, will change the way how the other substances distribute on them [7,8]. Similarly, for the formation of an ordered structure, the properties of the contacting surfaces have different effects on the morphologies of the ordered structures [9–12]. Crystal, as one of the most typical three-dimensional ordered structures, its lattice structure is also affected by external surface properties during the formation process. Many previous theoretical and experimental studies have worked to explore the relations between the external surface properties and the morphologies of the crystals, and some interaction mechanisms have been clarified. Under the homogeneous condition, the formed lattice structure is ideal and defect-free, but once there is a substance in the system that has the different physicochemical properties to the crystalline materials, it will cause lattice deformation and induce defects [13,14]. An external contacting surface would decide the morphologies and growth patterns of the crystal lattices growing on it. For example, surface roughness affects the crystal structure [15], and the difference in surface chemical interactions affects the growth direction of the lattice structure as well [16].

In these previous works, the influences of the external surfaces had been discussed and studied to a large extent. Some theoretical and simulation methods also have provided microscopic insights into dynamic processes of crystal formations [17,18]. However, the understanding of the microscopic mechanism is far from enough. For one reason, most crystal structures are at nanoscales and the structural units in a lattice, like atoms or molecules, are the

* Corresponding authors at: State Key Laboratory of Organic-Inorganic Composites, Beijing University of Chemical Technology College of Materials Science and Engineering, Beijing University of Chemical Technology Beijing 100029, China.
** Corresponding author.
E-mail addresses: houyq@xmu.edu.cn (Y. Hou), zhangch@mail.buct.edu.cn (C. Zhang), mijg@mail.buct.edu.cn (J. Mi).

https://doi.org/10.1016/j.cclet.2019.07.054
1001-8417/© 2019 Chinese Chemical Society and Institute of Materia Medica, Chinese Academy of Medical Sciences. Published by Elsevier B.V. All rights reserved.

observation objects which are smaller than the nanometer scale, which brings challenges for researchers to study the structural evolution from the accuracy of atomic scale. The other reason is that for crystals, how to represent reliably the oriented interactions between all structural units in lattices is still a challenge in effective theoretical studies.

Density functional theory (DFT) in the statistical mechanics is a powerful mean to study the behaviors of heterogeneous fluids [19,20]. Later, modified with the tensor version of White Bear II [21], it had been successfully applied to the studies of crystal structures [22,23]. Further, combining DFT with the diffusion equation, we got the dynamic density functional theory (DDFT) [24,25], which can predict the metastable structures and their dynamic evolutions over time. Through the DDFT method, the formation and evolution processes of different ordered structures were studied [26]. Studies had shown that the structure of the nucleus plays a decisive role in the final morphology of the crystal lattice [27], and different external surfaces provide different inducing effects, further inducing crystal structures with different growth directions [16].

Speculated by these splendid works, we found that the oriented interaction is the internal driving force for the formation of crystal structures. In the process of water freezing, we introduced the directionality of hydrogen bonds to provide the oriented interactions and successfully reproduced the phase transition from water to ice [28]. Similarly, the deformation and self-healing properties of the FCC lattice around an impurity particle were successfully demonstrated by introducing the oriented interactions [29]. All of these previous works have laid the foundation for combining the DDFT theory with the method of introducing oriented interactions and extending it to studying a more complex system with chain molecular structure. Taking polyethylene (PE) as an example, we try to extend the DDFT approach to exploring PE crystal, a most typical crystalline polymer, to obtain deep insight into its microscopic defect morphologies when it is interacting with different surfaces from the accuracy of the CH_2 groups.

The structure of a PE lattice is shown in Fig. 1a. The PE molecular chains are arranged in a planar sawtooth sequence in an orthorhombic lattice. To simplify the model, we coarsened each CH_2 group into a sphere α with the diameter of σ_α, so that the entire molecular chain is simplified into a series of tangent beads, as shown in Fig. 1b. Based on the above coarse-grained model, we used the DDFT theoretical framework to study the formation of ordered structures and defects in the PE lattice around different surfaces. The spatial distribution of CH_2 groups evolving over time can be described by the following equation (Eq. 1) [30]:

$$\frac{\partial\rho(\mathbf{r},t)}{\partial t} = D\nabla_{\mathbf{r}}\cdot\left\{\rho(\mathbf{r},t)\nabla_{\mathbf{r}}\frac{\delta F[\rho(\mathbf{r},t)]}{\delta\rho(\mathbf{r},t)}\right\} \tag{1}$$

where t denotes the time evolution, D is the diffusion constant of CH_2 groups and keep constant during the dynamic process. $\tau_B = \sigma_\alpha^2/D$ is chosen as the time unit. The dynamic processes were kept with a finite time step of $\Delta t = 10^{-4}\tau_B$. After calculation of N steps, the time reached $t = \Delta t\cdot N = 10^{-4}\times N\cdot\tau_B$. $\rho(\mathbf{r},t)$ indicates the density distribution of the CH_2 groups in PE lattices as a function of position $\mathbf{r}$ and time t. The total Helmholtz free energy $F[\rho(\mathbf{r},t)]$ depends on the density distribution $\rho(\mathbf{r},t)$ and can be separated into three components (Eq. 2) [31]

$$\begin{aligned}F[\rho(\mathbf{r},t)] &= k_BT\int d\mathbf{r}\rho(\mathbf{r},t)\{\ln[\rho(\mathbf{r},t)]-1\}\\ &+F^{\mathrm{ex}}[\rho(\mathbf{r},t)]+\int d\mathbf{r}\rho(\mathbf{r},t)V_{\mathrm{ext}}(\mathbf{r},t)\end{aligned} \tag{2}$$

to represent the contributions of ideal reference, excess free energy, and external potentials $V_{\mathrm{ext}}(\mathbf{r},t)$ given by the external surfaces. Here k_B is the Boltzmann constant, and T is the temperature. For PE chains in lattice, the excess free energy $F^{\mathrm{ex}}[\rho(\mathbf{r},t)]$ can be further decomposed into four contributions (shown as Eq. 3), which are hard-sphere repulsion $F^{\mathrm{hs}}[\rho(\mathbf{r},t)]$, dispersive attraction $F^{\mathrm{att}}[\rho(\mathbf{r},t)]$, chain constrain $F^{\mathrm{chain}}[\rho(\mathbf{r},t)]$, and bond angle bending $F^{\mathrm{angle}}[\rho(\mathbf{r},t)]$, that is,

$$\begin{aligned}F^{\mathrm{ex}}[\rho(\mathbf{r},t)] &= F^{\mathrm{hs}}[\rho(\mathbf{r},t)]+F^{\mathrm{att}}[\rho(\mathbf{r},t)]\\ &+F^{\mathrm{chain}}[\rho(\mathbf{r},t)]+F^{\mathrm{angle}}[\rho(\mathbf{r},t)]\end{aligned} \tag{3}$$

Here, dispersive attraction $F^{\mathrm{att}}[\rho(\mathbf{r},t)]$ indicates the non-bond interactions among different CH_2 groups in PE lattice and can be expressed as follow (Eq. 4):

$$F^{\mathrm{att}}[\rho(\mathbf{r},t)] = -\frac{1}{2}\int d\mathbf{r}\int d\mathbf{r}'\rho(\mathbf{r},t)\rho(\mathbf{r}',t)c^{\mathrm{att}}_{\mathrm{orient}}(|\mathbf{r}-\mathbf{r}'|) \tag{4}$$

The spatial structure of this interaction potential is not only related to the strength of the interactions, but also the relative positions of the closest CH_2 groups in lattice. It should be pointed out that different crystal structures have different oriented interactions and therefore have the unique direct correlation functions $c^{\mathrm{att}}_{\mathrm{orient}}(\mathbf{r})$ with orientation characteristics. In the small molecular or simple crystals studied previously, such as BCC crystal illustrated in Fig. 2a, the forces acting on the structural units at different locations in the BCC lattice are equivalent, which means they all have the same $c^{\mathrm{att}}_{\mathrm{orient}}(\mathbf{r})$. In PE lattice, however, due to the zigzag chain conformation, the different CH_2 groups in the same chain are not equivalent in orientation anymore and can be divided into four different types, as shown in Fig. 2b. According to the types of groups in PE lattice, four kinds of oriented direct correlation functions $c^{\mathrm{att}}_{\mathrm{orient,i}}(\mathbf{r})$, $i = 1,2,3,4$ are defined to represent different oriented interactions. Therefore, each CH_2 group processes its own $c^{\mathrm{att}}_{\mathrm{orient,i}}(\mathbf{r})$, which embraces the information of the spatial topology of PE chain in crystal lattice, shown in Fig. 2c. Therefore, the oriented interactions between different CH_2 groups are described by the following equation (Eq. 5).

$$F^{\mathrm{att}}[\rho(\mathbf{r},t)] = -\frac{1}{2}\sum_{i=1}^{4}\int d\mathbf{r}\int d\mathbf{r}'\rho_i(\mathbf{r},t)\rho_i(\mathbf{r}',t)c^{\mathrm{att}}_{\mathrm{orient,i}}(|\mathbf{r}-\mathbf{r}'|) \tag{5}$$

The specific expansions of other excess free energies are expanded in Supporting information in more detail. Based on this free-energy expression, the optimum parameters of the PE lattice can be determined by minimizing the value of the free energy and the results are shown in Fig. 1c. The steps of the optimizations are given in Supporting information.

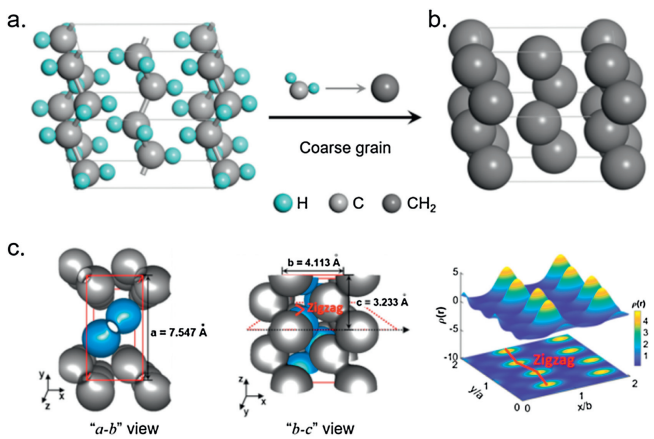

Fig. 1. The schematic presentation of PE ($1\times1\times2$) unit cells. (a) The original structure of PE lattice. (b) The coarse-grained model of PE lattice. (c) The "*a-b*" view, "*b-c*" view and two-dimensional cut of density distribution in (001) plane of the optimum lattice structure.

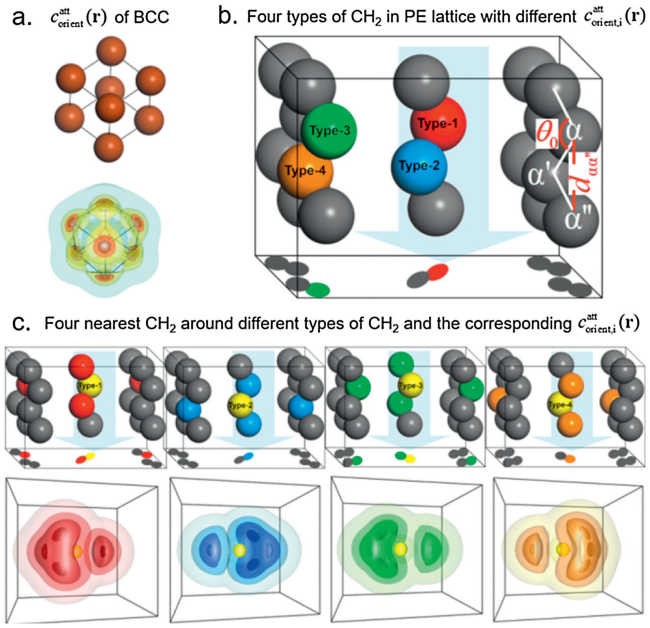

Fig. 2. Different types of $c^{att}_{orient}(\mathbf{r})$ in BCC and PE lattice. (a) Four nearest atoms around the body-centered atom and the three-dimensional contour plots of the corresponding $c^{att}_{orient}(\mathbf{r})$ in BCC. (b) Four types of CH_2 groups with different orientations are labeled. Projection of the periodic structure along the direction of chain axes is shown on the bottom. (c) The yellow spheres are the reference groups, around which the four nearest CH_2 are depicted. The corresponding $c^{att}_{orient,i}(\mathbf{r})$ are plotted in three-dimensional contour plots with the gradient colors of heavier color indicating higher degree of orientation.

The reliability of the current theoretical approach was verified by comparing the theoretical predictions with experimental phase equilibrium data. More details are displayed in Supporting information. The effects provided by the contact surfaces can be introduced as the external field potentials $V_{ext}(\mathbf{r},t)$ and the deformations and evolutions of the morphologies of PE lattices are further discussed one by one in the following parts.

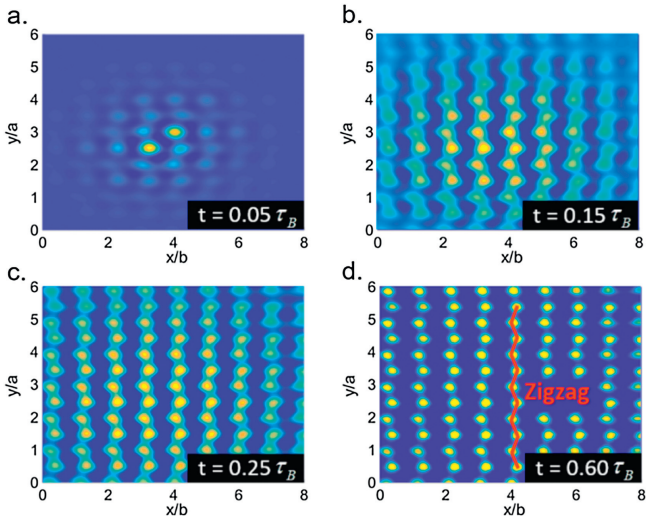

Fig. 3. The "*a*-*b*" views of density distributions of PE lattice at different moments (a) $t = 0.05\tau_B$, (b) $t = 0.15\tau_B$, (c) $t = 0.25\tau_B$, (d) $t = 0.60\tau_B$ of crystal growth without contacting the external surface. In order to show the structure more clearly, only 8×6 repetition periods are intercepted and displayed. Each bright point represents a position of CH_2, and the CH_2 groups along the "*a*" direction in the defect-free lattice distribute in zigzag form, which will be used as an indicator to determine whether the final structures are defect-free lattices.

Firstly, theoretically, it is possible to produce a defect-free PE lattice without the intervention of any external surfaces. Fig. 3 shows the evolution of the PE lattice formed without contacting any external surfaces. Four typical snapshots are depicted. In initial stage (Fig. 3a, $t = 0.05\tau_B$), the two bright yellow areas are the initial density fluctuations which are externally imposed as thermal fluctuations, induced by which the surrounding CH_2 groups begin to fluctuate. As the fluctuation increases (Fig. 3b, $t = 0.15\tau_B$), the chains start to regulate their architectures to form an ordered arrangement, which is driven by the oriented interactions. As the time goes by, more and more CH_2 groups are arranged in the crystal lattice, then PE lattice gradually appears. Thereafter, the PE lattice grows layer by layer (Fig. 3c, $t = 0.25\tau_B$). In the end, the calculation space is full of PE lattice through the self-assembly process of CH_2 (Fig. 3d, $t = 0.60\tau_B$). In the final distribution of density peaks, the regular zigzag lines formed along the "*a*" axis, which reveals the defect-free structure of the PE lattice.

Secondly, a flat inert surface is introduced, which produces the external field potential that can be expressed as (Eq. 6):

$$V_{ext}(\mathbf{r},t) = \begin{cases} 0 & \mathbf{r} \geq \sigma_\alpha \\ \infty & \mathbf{r} < \sigma_\alpha \end{cases} \quad (6)$$

It can be seen from the Eq. 6 that when the PE chains contact the surface, they will be subjected to an infinite repulsive force. That is to say, the PE chains cannot enter the inside of the surface. At the same time, when it is away from the surface, the force acting on the CH_2 groups becomes zero, indicating that the surface does not exert any chemical attractions on the CH_2 groups. The $V_{ext}(\mathbf{r},t)$ is shown in Fig. 4a. Around this inert flat surface, the CH_2 groups are gradually arranged in order, and finally the formed lattices get deformations. Different snapshots descriptions at different moments during the dynamic process are displayed in Supporting information. As can be seen from the "*a*-*b*" view of the final structure in Fig. 4b, the original zigzag line is deformed into a straight line and form the lamellar structure near the flat surface. Due to the inertness of the flat surface, the density on the surface is lower than that in the bulk region, which means the probability of the density distribution around the inert surface is low. However, with increasing distance from the surface, the ordered structure transforms gradually from the lamellar layers to the defect-free crystal structure. The PE crystal shows the self-healing ability. It

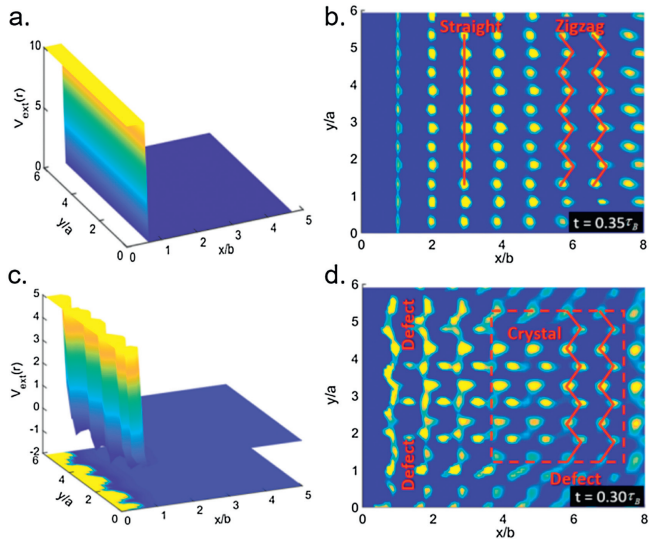

Fig. 4. The external potential exerted by (a) a flat inert surface and (b) the corresponding defect morphology. The external potential exerted by (c) a compatible surface and (d) the corresponding defect morphology.

can be seen that the influence of such an inert flat surface on the PE lattice mainly exists in the shape of the defects.

Thirdly, what if the surface is no longer inert, but has better compatibility with the PE molecular? For the sake of simplicity, we constructed an external surface with the same composition as the PE molecular, in which the CH_2 groups are randomly distributed. Such surface will have better compatibility with PE and thus generate stronger chemical interactions. The potential field generated by it can be obtained by integrating the pair interaction potentials between the CH_2 α in PE crystal and site p in the external surface (Eq. 7),

$$V_{\mathrm{ext}}(\mathbf{r},t)=\begin{cases}\sum_{\mathrm{p}}4\varepsilon_{\alpha\mathrm{p}}\left[\left(\frac{\sigma_{\alpha\mathrm{p}}}{\mathbf{r}}\right)^{12}-\left(\frac{\sigma_{\alpha\mathrm{p}}}{\mathbf{r}}\right)^{6}\right] & \mathbf{r}\geq\sigma_{\alpha\mathrm{p}}\\ \infty & \mathbf{r}<\sigma_{\alpha\mathrm{p}}\end{cases} \quad (7)$$

in which $\varepsilon_{\alpha\mathrm{p}}$ and $\sigma_{\alpha\mathrm{p}}$ are the Lennard-Jones parameters for different sites, which are calculated using the Lorentz-Berthelot mixing rules with $\sigma_{\alpha\mathrm{p}}=(\sigma_{\alpha}+\sigma_{\mathrm{p}})/2$ and $\varepsilon_{\alpha\mathrm{p}}=(\varepsilon_{\alpha}\cdot\varepsilon_{\mathrm{p}})^{1/2}$. The result is shown in Fig. 4c. One can see that there is a potential well generated near the surface and the depth of the well represents the strength of the chemical interactions.

The final morphology of PE crystal around the compatible surface is obtained and shown in Fig. 4d. The lattices near the surface are badly damaged but a relatively defect-free structure of PE lattice emerges away from the surface over five layers. Such structure can be attributed to the surface properties. Physically, due to the external force field provided by amorphous surface distributing randomly, the density distribution of PE chains near the surface is irregular, resulting in an irregular lattice morphology. In terms of chemistry, in the vicinity of the surface, PE tends to aggregate in the areas with strong interactions to the surface, leading to increasing probability to self-assemble into the ordered crystal. While in the areas with weak interactions, the density distribution shows some degree of order but is not enough to form the crystal structure. As the distance increases, the influence of the surface is rapidly attenuated, a relatively defect-free crystal lattice shows again. In this way, the PE lattices growing on the compatible surface get a specific micromorphology that some defect-free PE lattices coexist with other defective lattices, and the distribution of the defect regions is affected by the roughness of the external surface.

In the perspective of the duration, the length of time required to obtain the final equilibrium structures indirectly reflects the speed of the entire dynamic process. The total time needed for the formation of PE lattice in the bulk phase is $0.60\tau_{\mathrm{B}}$ that is longer than that around the inert surface $0.35\tau_{\mathrm{B}}$, and the total time is $0.30\tau_{\mathrm{B}}$ that is much shorter around the compatible surface. The formation speed increases obviously when the external surfaces exist. The external interactions promote the initial density fluctuations and accumulations so that more CH_2 groups can accumulate quickly, thus accelerate the whole arrange process. Moreover, the formation speed on the compatible surface is faster than that on the inert surface, which can be attributed to the stronger chemical interactions between the PE lattices and the surface. Better compatibility makes PE chains easier to aggregate on the surface in a short time and realize a faster disorder-order transition.

To sum up, through the comparison of the three conditions above, one can see that in the absence of the external surfaces, the only kind of force acting on the CH_2 groups are the oriented interactions which drive the CH_2 groups to arrange into the defect-free lattice. However, when there is an external surface, rarely the external force fields are perfectly compatible with the thermodynamically favored defect-free crystal structures, then the kinds of the force acting on the CH_2 are not only the oriented interactions but also the inducing forces produced by the external surfaces. The physical interactions mainly affect the spatial distribution of the defect regions, and the chemical interactions mainly affect the strength of the interactions between the external surfaces and the PE lattice, further affect the density distribution and formation speed of the PE lattice. Therefore, the physical and chemical interactions contribute synergistically to determine the final morphology of the PE crystal, which is also the result of competition between the internal oriented interactions of lattices and the external inducing forces of surfaces. The conclusions may provide some guidance for controllable preparation of the lattice structures by regulating the physical and chemical properties of the external surfaces.

Acknowledgments

This work was supported by the National Natural Science Foundation of China (Nos. 21476007, 21673197, 21621091), the National Key R&D Program of China (No. 2018YFA0209500), the 111 Project (No. B16029), the Fundamental Research Funds for the Central Universities of China (No. 20720190037), the Natural Science Foundation of Fujian Province of China (No. 2018J06003), the Special Project of Strategic Emerging Industries from Fujian Development and Reform Commission, and Chemcloudcomputing of Beijing University of Chemical Technology.

Appendix A. Supplementary data

Supplementary material related to this article can be found, in the online version, at doi:https://doi.org/10.1016/j.cclet.2019.07.054.

References

[1] E.B. Trigg, T.W. Gaines, M. Maréchal, et al., Nat. Mater. 17 (2018) 725–731.
[2] L. Wen, K. Xiao, A.V.S. Sainath, et al., Adv. Mater. 28 (2016) 757–763.
[3] Z. Zhang, L. Wen, L. Jiang, Chem. Soc. Rev. 47 (2018) 322–356.
[4] Z. Zhang, X.Y. Kong, G. Xie, et al., Sci. Adv. 2 (2016) e1600689.
[5] P.B. Bowden, R.J. Young, J. Mater. Sci. 9 (1974) 2034–2051.
[6] A. Tracz, I. Kucińska, J.K. Jeszka, Macromolecules 36 (2003) 10130–10132.
[7] M. Annamalai, K. Gopinadhan, S.A. Han, et al., Nanoscale 8 (2016) 5764–5770.
[8] M. Cao, Z. Li, H. Ma, et al., ACS Appl. Mater. Interface 10 (2018) 20995–21000.
[9] Y. Diao, T. Harada, A.S. Myerson, T.A. Hatton, B.L. Trout, Nat. Mater. 10 (2011) 867.
[10] T. Tsuruoka, K. Inoue, A. Miyanaga, et al., J. Cryst. Growth 487 (2018) 1–7.
[11] A.J. Page, R.P. Sear, J. Am. Chem. Soc. 131 (2009) 17550–17551.
[12] H. Li, S. Yan, Macromolecules 44 (2011) 417–428.
[13] S. Suresh, Nat. Mater. 5 (2006) 253–254.
[14] Y.N. Palyanov, Y.M. Borzdov, A.F. Khokhryakov, I.N. Kupriyanov, A.G. Sokol, Cryst. Growth Des. 10 (2010) 3169–3175.
[15] A. Jabbarzadeh, X. Chen, Faraday Discuss. 204 (2017) 307–330.
[16] T. Neuhaus, M. Schmiedeberg, H. Löwen, New J. Phys. 15 (2013) 073013.
[17] K.R. Elder, M. Katakowski, M. Haataja, M. Grant, Phys. Rev. Let. 88 (2002) 245701.
[18] A. Bourque, C.R. Locker, G.C. Rutledge, Macromolecules 49 (2016) 3619–3629.
[19] R. Evans, Adv. Phys. 28 (1979) 143–200.
[20] R. Evans, Density functionals in the theory of nonuniform fluids, in: D. Henderson (Ed.), Fundamentals of Inhomogeneous Fluid, Marcel Dehker Inc, New York, 1992.
[21] Y. Rosenfeld, Phys. Rev. Lett. 63 (1989) 980.
[22] Y. Chang, J. Mi, C. Zhong, J. Chem. Phys. 140 (2014) 204706.
[23] J. Feng, H. Zhou, X. Wang, J. Mi, J. Phys. Chem. C 120 (2016) 8630–8639.
[24] J.G.E.M. Fraaije, J. Chem. Phys. 99 (1993) 9202–9212.
[25] N.M. Maurits, J.G.E.M. Fraaije, J. Chem. Phys. 107 (1997) 5879–5889.
[26] T. Neuhaus, A. Härtel, M. Marechal, M. Schmiedeberg, H. Löwen, Eur. Phys. J. Spec. Top. 223 (2014) 373–387.
[27] S. van Teeffelen, C.N. Likos, H. Lowen, Phys. Rev. Lett. 100 (2008) 108302.
[28] Y. Ye, N. Ning, M. Tian, L. Zhang, J. Mi, Cryst. Growth Des. 17 (2016) 100–105.
[29] Y. Hou, Y. Ye, Z. Du, C. Zhang, J. Mi, J. Phys. Chem. C 121 (2017) 23763–23768.
[30] M. Rex, H. Lowen, Phys. Rev. Lett. 101 (2008) 148302.
[31] H. Löwen, M. Heinen, Eur. Phys. J. Spec. Top. 223 (2014) 3113–3127.